Jurnal Teknologi, 47(A) Dis. 2007: 35–53

THE EFFECT OF DIAPHRAGMS IN CONTINUOUS SILL MEMBER ON THE STRENGTH OF AUTOMOTIVE B-PILLAR

TAN CHEE FAI[1] & MOHD. RADZAI SAID[2]

Abstract. The competing factors in automotive engineering design may be divided into four main categories: cost, performance, safety, and fuel economy. All four are related by vehicle weight considerations. As far as cost is concerned, heavy vehicle weight is a waste of money, but, if overall volume is not to be reduced, reducing vehicle weight can be more expensive. Lighter vehicles have better fuel efficiency. Furthermore, in improving the safety of passengers in collision, it will be of benefit to decrease the load that occurs during the collision. The paper discusses the knowledge on the behaviour of T-frame structure under specific loading will be obtained by experimental methods in order to investigate the deflection of the vehicle B-pillar or T-frame structure. In addition, a series of T-frame structure as designed with inner diaphragms at various locations in the sill member in order to investigate the effect of inner diaphragm and continuous sill member. Finite element analysis and experimental test were carried out on the in-plane bending. The results from both methods are compared and examined.

Keywords: Vehicle T-frame, diaphragms, continuous sill member, experimental methods, finite element analysis, in-plane bending

Abstrak. Faktor persaingan dalam reka bentuk kejuruteraan automotif boleh dibahagi kepada empat kategori utama: kos, prestasi, keselamatan, dan penggunaan bahan api. Keempat-empat faktor ini ada kaitannya dengan berat kenderaan. Sekiranya kos dipertimbangkan, berat yang berlebihan merupakan satu pembaziran wang, tetapi, jika isipadu keseluruhan tidak dikurangkan, pengurangan berat kenderaan adalah lebih berkos tinggi. Kenderaan yang lebih ringan mempunyai penjimatan bahan api yang lebih baik dan melindungi alam sekitar. Tambahan pula, dalam meningkatkan keselamatan penumpang semasa perlanggaran, kenderaan ringan dapat mengurangkan beban maksimum yang terjadi semasa perlanggaran. Kertas ini membincangkan pengetahuan terhadap sikap struktur kerangka-T di bawah bebanan khas yang diperoleh melalui kaedah uji kaji bagi menyiasat pesongan pada kenderaan tiang-B atau struktur kerangka-T. Selain itu satu siri kerangka-T telah direka dengan diafragma dalaman di lokasi yang berlainan di dalam anggota ambang yang bertujuan untuk menyiasat tindak balas diafragma dalaman dan bahagian ambang yang bersambungan. Analisis unsur terhingga dan ujian eksperimen dijalankan ke atas pesongan dalam permukaan. Keputusan daripada kedua-dua kaedah ini dibanding dan dikaji.

Kata kunci: Kerangka-T kenderaan, diafragma, bahagian ambang bersambungan, kaedah uji kaji, analisis unsur terhingga, pesongan dalam permukaan

[1] Designed Intelligence Group, Faculty of Industrial Design, Technische Universiteit Eindhoven, P. O. Box 513, 5600 MB Eindhoven, The Netherlands. Tel: +31-40247 2514 E-mail: c.f.tan@tue.nl

[2] Faculty of Mechanical Engineering, Universiti Teknikal Malaysia Melaka, Locked Bag 1200, Hang Tuah Jaya, 75450 Ayer Keroh, Melaka, Malaysia.

1.0 INTRODUCTION

The framework of the automotive body structure is comprised of thin walled section members in the formed of overlapping sheet metal fastened by spot-welds. In analyzing the structure of the vehicle body, it is assumed that the intersecting angles at which members are joined together, varies according to the external forces. The automotive frame joints are subjected to dynamic and static loads. The dynamic analysis can be carried out using matrix methods provided the overall stiffness. The mass distribution is known but it is quite difficult to find a suitable approach to determine damping properties. The static analysis can be used to find the force-displacement relationships of the structure. Static analysis, in general, includes the calculation of deformations and internal forces such as bending moments, torque, bi-moments, longitudinal and shear forces. Experiments and finite element analysis can determine joint rigidity. Although this framework is accounting for only a small part by weight of the entire vehicle but it exerts a substantial effect on the response of the vehicle structure.

The effective design of the vehicle T-frame structure will maximise the safety of the passengers and reduce the vehicle weight. It is true that the automotive industries have been working hard to reduce the vehicle weight in order to achieve better fuel efficiency. Furthermore, in improving the safety of passengers in a collision, it will be benefit to decrease the load that occurs during the collision. This can reduce the level of occupant's injury and control the deformation of the structure to ensure a sufficient safe space for occupant.

Therefore, in order to reduce the vehicle body weight and yet maintaining satisfactory function, performance and engineering reliability, it is extremely important to establish a consistent procedure in analyzing and evaluating the frame joint and to have fundamental knowledge about the behaviour of joints under loads. A point to be noted is that although the frame joints are only a small part of the entire vehicle, they exert a great influence on the structure system.

The goal of this work is to describe the designed of inner diaphragm into the automotive T-frame structure in several locations on continuous sill member. The specimens were employed to show the effects of different location of inner diaphragm and in continuous sill member on the stiffness of T-frame structure. A mechanical test rig was designed and manufactured in order to test the T-frame. Experimental test and finite element analysis were carried out and compared.

2.0 RELATED WORK

Most of the research involving joint stiffness of the automotive body structure related to thin-walled structures in which the studies are on fastened method, flexible characteristics, collapse behaviour, torsional problems and stress distributions. These studies were conducted because the frame joints give a very important affect on the

vehicle response. In addition, most of the studies found that the stiffness of the frame joints greatly influenced on the overall stiffness of the vehicle body structure.

McGregor *et al.* [1] developed a joint design approach for adhesively bonded and spot welded aluminium automotive structures. The approach includes an allowance for joint geometric variables, manufacturing variability and complex joint loading. An important aspect in the development of the approach is to minimize the detail required to model the joints in a full vehicle model. The accuracy of the approach is demonstrated on a simple structure subjected to complex loading, and the use of the approach is illustrated on a full vehicle.

Sunami *et al.* [2, 3] performed their analysis on the joint rigidity of the automotive body structure both in in-plane and out-of-plane bending of plane joint structures. They have made a fundamental study of the joint rigidity involving T- or L-shaped thin walled box beams and examining several factors that caused the rigidity to be reduced. They used a theoretical equation i.e. the theory of shear flow and the results confirmed by experimental values. For the in-plane study, they have concluded that the joint rigidity of box beams depends on the "release" (insufficient constrained condition) and shearing deformation and elongation of joints. From this study also they have pointed out that the analysis of fundamental behaviour of joints can be used as a step to plan structural designs. Sharman and Al-Hammoud [4] carried out a comprehensive study to determine the effect of local details on the stiffness of car body joint. Three joints between the structural members meeting the roof of a small car were tested for stiffness in the plane of the side frame.

Niisawa *et al.* [5] performed an analytical method of rigidities of thin-walled beams with spot welding joints and its application to torsion problems. In their study, they have discussed the elastic properties of the spot welding joints in the transmission of the shearing forces and developed the method based on shear flow theory in introducing the elastic properties of spot welding joints into the structural analysis of thin-walled beams. Vayas and Briassoulis [6] developed a method for calculating the carrying capacity and the deformation characteristics of the joints. Static and kinematic limit state models are presented which allow the ultimate strength to be determined from closed formulae.

El-sayed [7] calculated the torsional spring rates of structural joints using finite elements. Balch and Steele [8] performed an asymptotic analysis for T-joint box beam structures. They discussed the decay distance of end effects of thin-walled box beams. Altenbach [9] and Altenbach *et al.* [10] presented a generalized theory of thin-walled beams with closed and open cross-sections using n degrees of freedom. The theoretical framework allows the solution of various application problems including T-joint box beam structures and vibrations.

For the finite element analysis, Shakourzadeh *et al.* [11] dealt with the finite element formulation for the analysis of space frames. A numerical method is presented to take into account the deformation of the joint connections in linear, non-linear and

stability analyses of three-dimensional thin walled beam structure. Moon *et al.* [12] presented a joint modelling methodology where the definition and assumptions of the joint are discussed. In addition, the joint stiffness analytical model is proposed using static load test results and also presented the sensitivity analysis method and a joint stiffness-updating algorithm. To verify these methods, the FE analysis results of a half size structural model of an automobile with rigid joints and rotational spring joints are compared with experimental analysis results. Mirza *et al.* [13] proposed the finite element formulation to incorporates rectangular plate and edge boundary spring elements. The model is then used to determine the punching shear and rotational stiffness of both double chord T-joints and single chord T-joints, thus demonstrating its versatility. The numerical values obtained are in good agreement with the experimental results available in the open literature.

Cheng and Deng [14] investigated the numerical performance of general shell elements in modelling spot-welded joints. Finite element meshes composed of purely three-dimensional (3D) elements and purely general shell elements are used to analyze the stress and deformation fields in a symmetric coach-peel spot-welded specimen and their solutions are compared in detail. It is found that a properly refined finite element mesh of general shell elements can produce stress and deformation solutions comparable to those generated by a similarly refined mesh of 3D solid elements. The findings of this paper have direct implications to the analysis of sheet metal structures with spot-welded joints (such as automotive structures).

3.0 FUNDAMENTAL ASPECT OF THE SPECIMEN

The cold rolled mild steel sheet was used to construct the specimens. It consisted of five components that are the base plate, inner diaphragm (baffles), vertical member, horizontal member (sill) and the jointing member. Once constructed, it formed a T-frame member with 75 mm corner radius at the jointing area and with closed hat section members and spot welded along its flanges.

The base plate was a planar sheet with 1.2 mm thickness in the form of T-shape with 55 mm corner radius. The horizontal member is an open hat section with 20 mm flanges over the complete length and having the same thickness as the base plate. It is connected to the base plate by means of spot welds at the pitch distance of 50 mm. Before these two components are connected, the inner diaphragms are connected to their particular locations in the horizontal member by means of three spot welds at two equal pitches all the way round except the one that faces the base plate. This has been plug welded at two equal distances with the base plate. The purpose of having these holes and extension length is to build a box of cement block at each end so that it can be regarded as fixed ends.

The vertical member is connected to the base plate by means of spot welds. This assembly is connected to a connecting plate with dimensions of 180 mm $\times$ 180 mm $\times$ 10 mm at the top part of the assembly by means of CO_2 arc welding. The purpose

of having the connecting plate is ensuring that the vertical member will move as one entity when loads are applied.

The jointing member connects the base plate, vertical/horizontal member by means of spot welds, fillet welds, plug welds and CO_2 arc welds. Plug welds were used in any area where spot welding electrodes were not accessible due to the shape of the T-joint. Although the jointing member was designed as one piece, in actual case it is made from three pieces of steel which are joined by one CO_2 arc welding operation due to the lack of production tools. In production cars the hat section of the sill and 'B' post are formed in one pressing process.

3.1 Type of Specimen

In this work, a specimen has been constructed with three examples where it is using a continuous sill member. As refer to Figure 1, the inner diaphragms have been located in-line with the sides of B-pillar (AM1), at the weld line (AM2) and at the outside of the weld line (AM3). The information about the specimen as shown in Table 1. Figure 2 shows the design of the specimen.

Table 1 Specimen: continuous horizontal member

Specimen's Identity	**AM1**	**AM2**	**AM3**
Location of Baffles (Left and Right)	160 mm	272 mm	40 mm

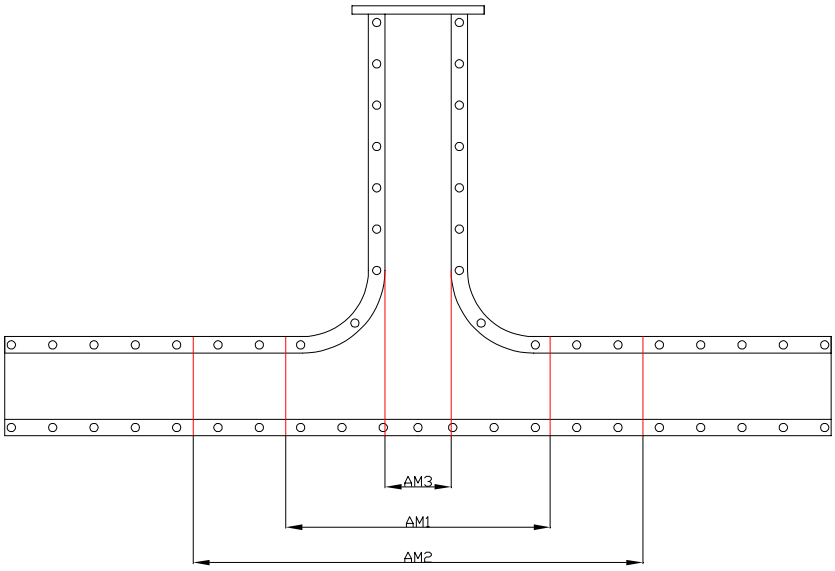

Figure 1 The location of the inner diaphragm

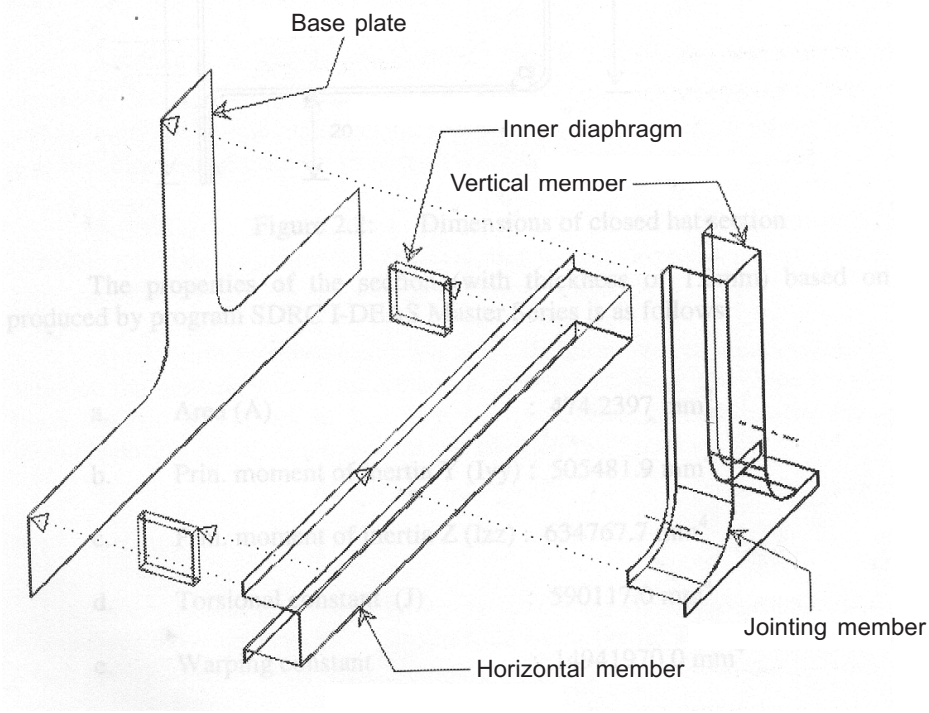

Figure 2 Parts of specimen

3.2 Experimental Testing

The in-plane bending case was considered in the experimental testing. The load applied at the top part of the vertical member and in parallel with the horizontal member (Figures 3, 4 and 5). The total displacement can be written as:

$$\delta_t = \delta_{VW} + \delta_{HW} + \delta_{HM} \quad (1)$$

Where

δ_t = Total displacement
δ_{VW} = Bending displacement of vertical member
δ_{HW} = Bending displacement of horizontal member
δ_{HM} = Rotation of the horizontal member

Based on these rotational assumptions, therefore through experimental test or finite element analysis, the stiffness of the joint can be easily obtained. Where through experimental test, the total displacement can be obtained, while the displacement of each member due to deformation of a beam can be calculated using beam theory or finite element analysis. In addition, the displacement at the loading point can be transformed into function, which includes the angular stiffness of the joint.

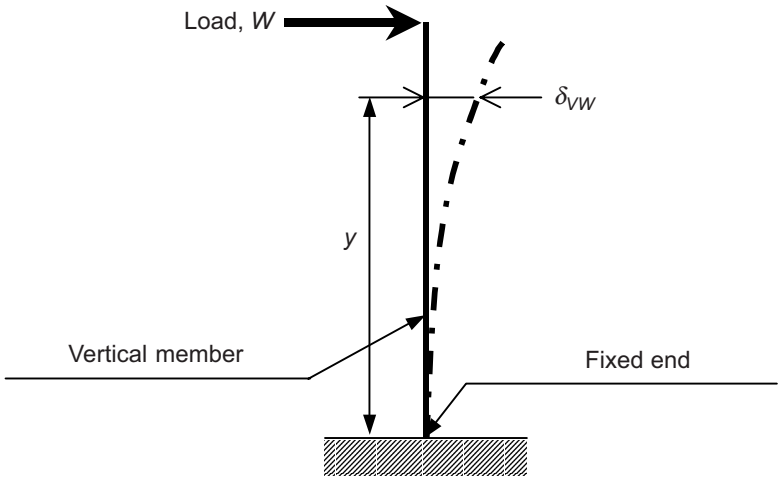

Figure 3 Vertical member as a cantilever

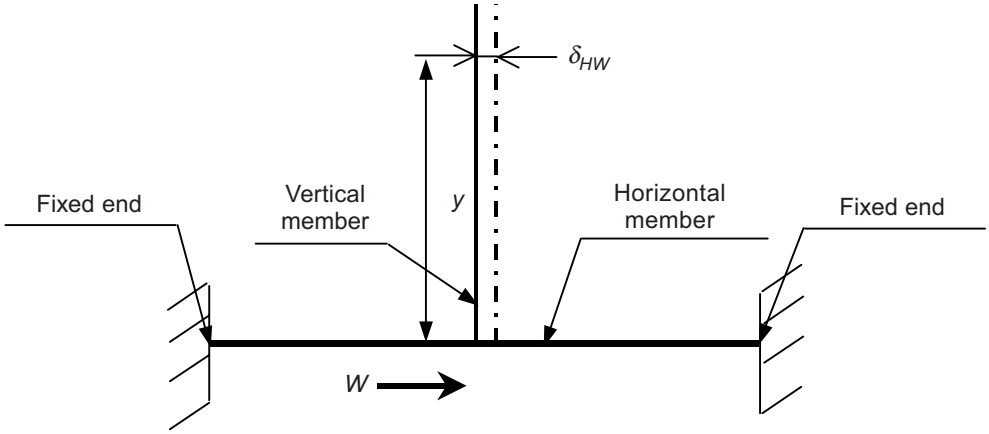

Figure 4 Horizontal member subjected to axial load, W

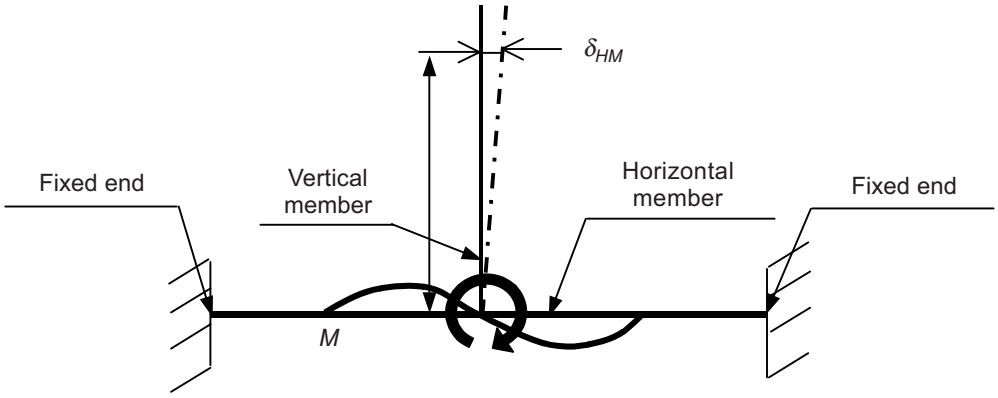

Figure 5 Horizontal member subjected to bending moment

To conduct the in-plane experimental testing, a mechanical test rig was designed and manufactured. The test rig also equipped with tensile gauge, turnbuckles, a clamping set, a Dexion frame and displacement gauges.

4.0 EXPERIMENTAL TEST RESULTS

For the in-plane bending test, 4 points were measured at the specimen. This points were represented by W, X, Y and Z (refer to Figure 6). Figure 7 shows the in-plane bending experiment on the test rig.

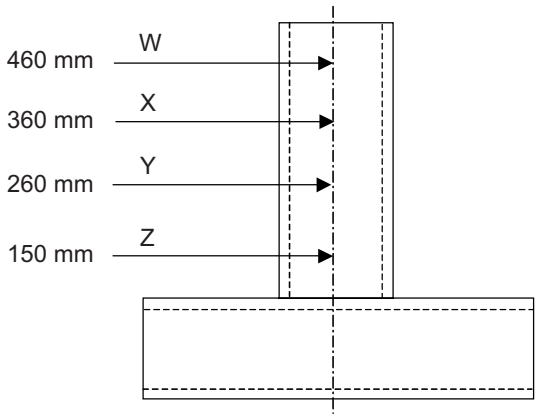

Figure 6 Location of points for experimental testing

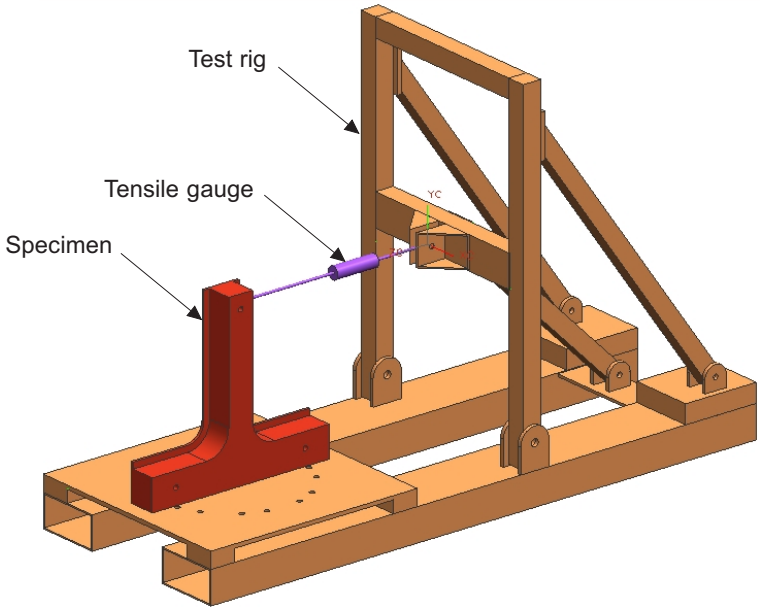

Figure 7 The in-plane bending experiment on the test rig

4.1 In-Plane Bending Test Result for Specimen AM1

Specimen AM1 is a continuous sill member with the diaphragms located at the weld line i.e. 160 mm left and right from the centreline of the T-frame structure. The linear of displacement with load occurred at point W, X, Y and Z is shown in Table 2 and plotted as in Figure 8.

Table 2 Results from specimen AM1

Location	Load (N)				
	180	360	540	720	900
W (460 mm)	0.034	0.085	0.138	0.19	0.46
X (360 mm)	0.024	0.058	0.095	0.13	0.162
Y (260 mm)	0	0.008	0.02	0.32	0.044
Z (145 mm)	0	–0.002	–0.004	–0.007	–0.01

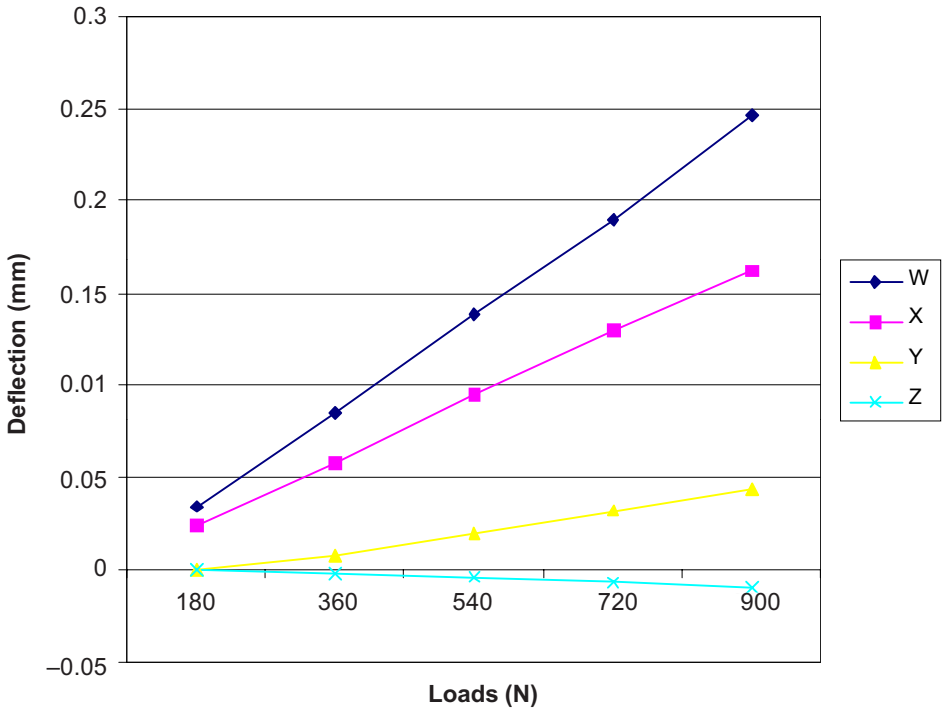

Figure 8 Deflection *vs.* load (Linearity Displacement)

The deflection against the load graph is constructed based on the maximum load's results (i.e. 900 N longitudinal load). Where the distance Z is at 145 mm from the bottom part of the T-frame i.e. the distance is measured from the lowest part based on

the centreline of the vertical member. The Y is located at 260 mm, X is at 360 mm and finally W is at 460 mm.

4.2 In-Plane Bending Test Result for Specimen AM2

This specimen is a continuous sill member with the diaphragms located at the outside of the weld lines i.e. 272 mm left and right from the centreline. The experimental results for AM2 as shown in Table 3 and Figure 9. Figure 9 show the deflection versus distance (location), where it is constructed based on maximum load applied.

Table 3 Results for model AM2

Location	**W (460 mm)**	**X (360 mm)**	**Y (260 mm)**	**Z (145 mm)**
Deflection	0.262	0.174	0.076	–0.008

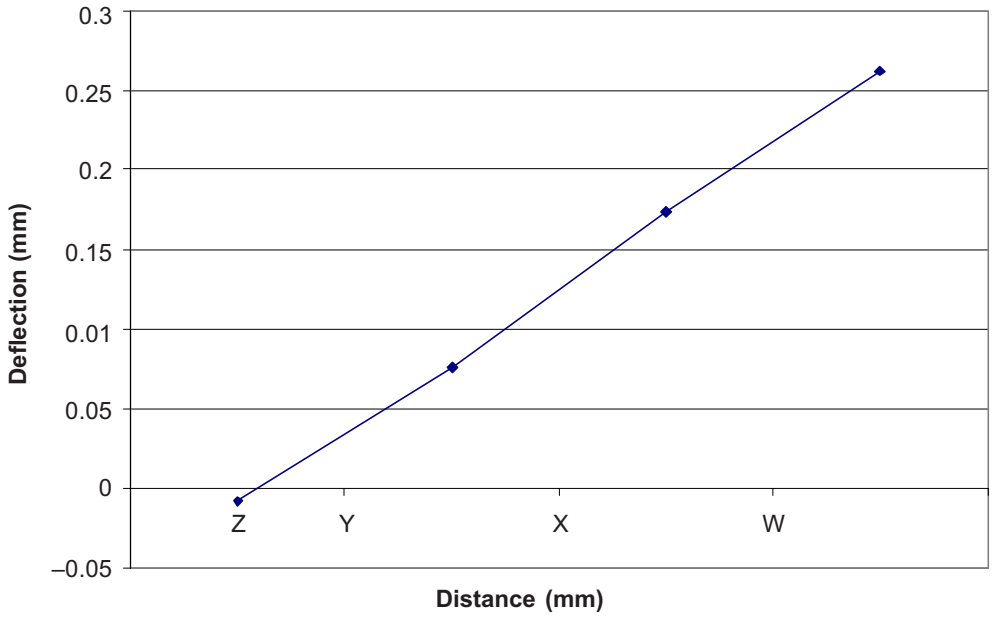

Figure 9 Deflection *vs.* Distance (AM2)

4.3 In-Plane Bending Test Result for Specimen AM3

The specimen is a continuous sill member with the baffles located in-line with the vertical member, i.e. 40 mm left and right from the centerline. The experimental results for AM3 as shown in Table 4 and Figure 10. The graph of deflection versus distance

Table 4 Results for model AM3

Location	W (460 mm)	X (360 mm)	Y(260 mm)	Z(145 mm)
Deflection	0.268	0.189	0.084	–0.008

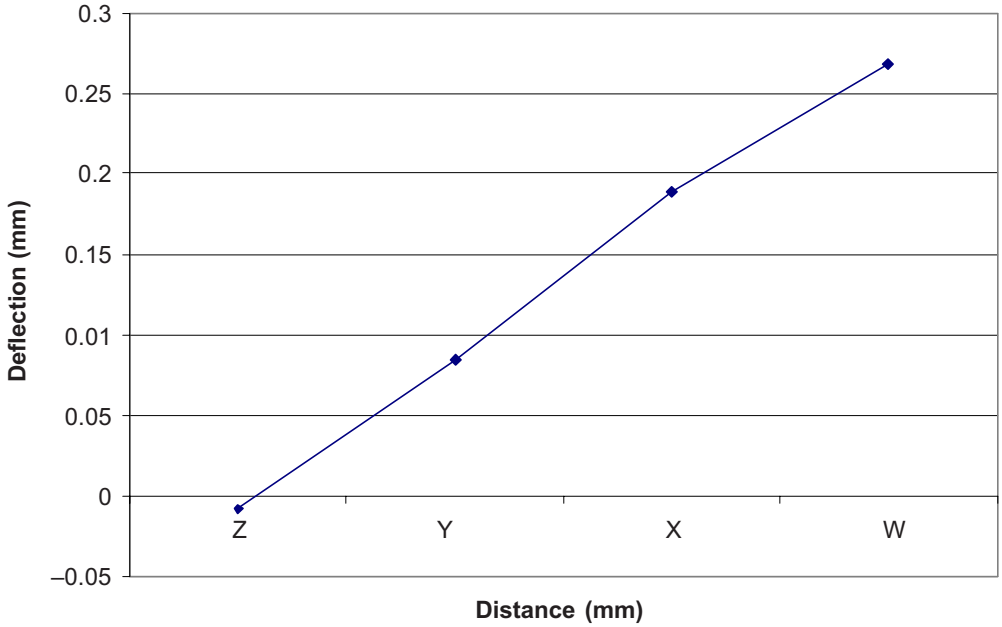

Figure 10 Deflection *vs* Distance (AM3)

(location) is constructed based on the maximum load applied. Figure 10 also shows that negative displacement existed at the joint region, i.e. point Z. This is the bowing effect due to compression.

4.4 Deflection of Vertical Member and Joint Region of Continuous Sill Member

The results obtained based on 900 N longitudinal load to specimens with continuous sill member have been tabulated as shown in Table 5 and Figure 11.

Based on Table 5 and Figure 11, the following are the pre-conclusion that can be made:

(i) Location of baffles on a continuous sill member does not give any major influence on the in-plane bending case. However, among these specimens, the specimen with inner diaphragms located at the weld line is stiffer than the inner diaphragms located with the side of B-pillar.
(ii) No 'match box' effect occurred in these types of specimens.

Table 5 Deflection of vertical member and joint region with continuous sill member

Location	W (460 mm)	X (360 mm)	Y(260 mm)	Z(145 mm)
AM1	0.246	0.162	0.044	–0.010
AM2	0.262	0.174	0.076	–0.008
AM3	0.268	0.189	0.084	–0.008

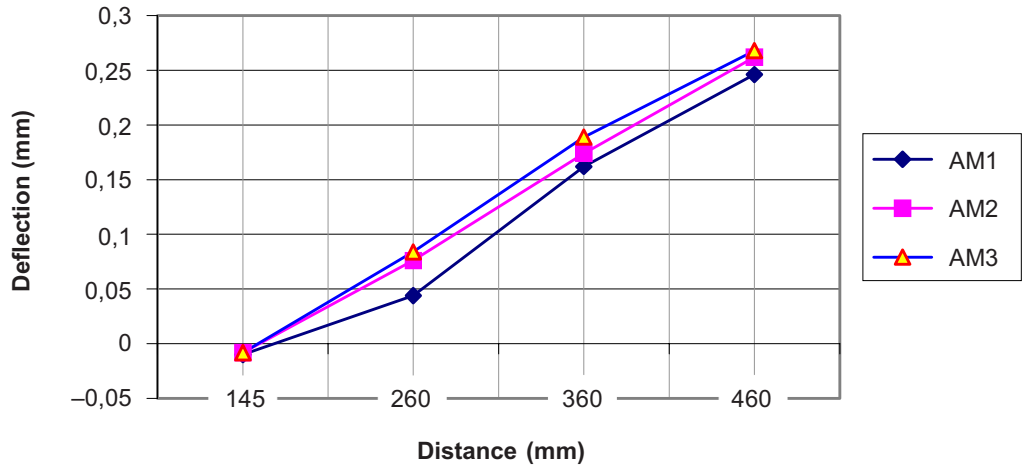

Figure 11 Deflection of vertical member and joint region of continuous sill member

5.0 FINITE ELEMENT ANALYSIS

The modelling of the specimen has been carried out in order to represent the actual joints of a vehicle and comparing its results with the results obtained from experimental testing. All of the finite element (FE) models consisted of four main parts, namely, base plate, vertical member, horizontal member and inner diaphragm (baffles). The model was created using square corner (i.e. no corner radii) in order to reduce the computational time.

The models were constructed using thin shell element without considering the solid modelling since the thickness of the plate is only 1.2 mm. Mapped meshed were used throughout the construction of the model in order to get better accuracy and moreover the model did not have any irregular shape. A four-nod simple rectangular element was used for mapped the meshing.

The top surface of the vertical member was constrained using a rigid element so that it can move as one unit when loads were applied. The base plate and the vertical member/horizontal member were connected by means of beam element (representing spot welds) at the pitch distance of 50 mm. The inner diaphragms are connected to their particular location in the horizontal member by means of three beam elements at two equal pitches all the way round. Both ends of the horizontal

member were fully restrained from any degree of freedom, which represent as fixed ends. Two forces were located along the edge (on the nodes) of the top surface of the vertical member (i.e. facing the direction of the force).

5.1 FE Results

For the FE analysis, the locations for the measurement are similar to the location as in Figure 6. The locations of the measurement are slightly deviates from the location as in Figure 6 because the location of the nodes is quite difficult to be on the same position. For this reason, the tolerance of ±5 mm has been given for the locations of the measurement.

5.1.1 Model AM1

The results obtained from the FE analysis are shown in Table 6 and Figure 12. The deformed model is shown in Figure 13. It can be seen that the joint region of the

Table 6 Results for model AM1

Location	W (456.6 mm)	X (358.9 mm)	Y(261.2 mm)	Z(143.6 mm)
Deflection	0.244	0.160	0.077	0.016

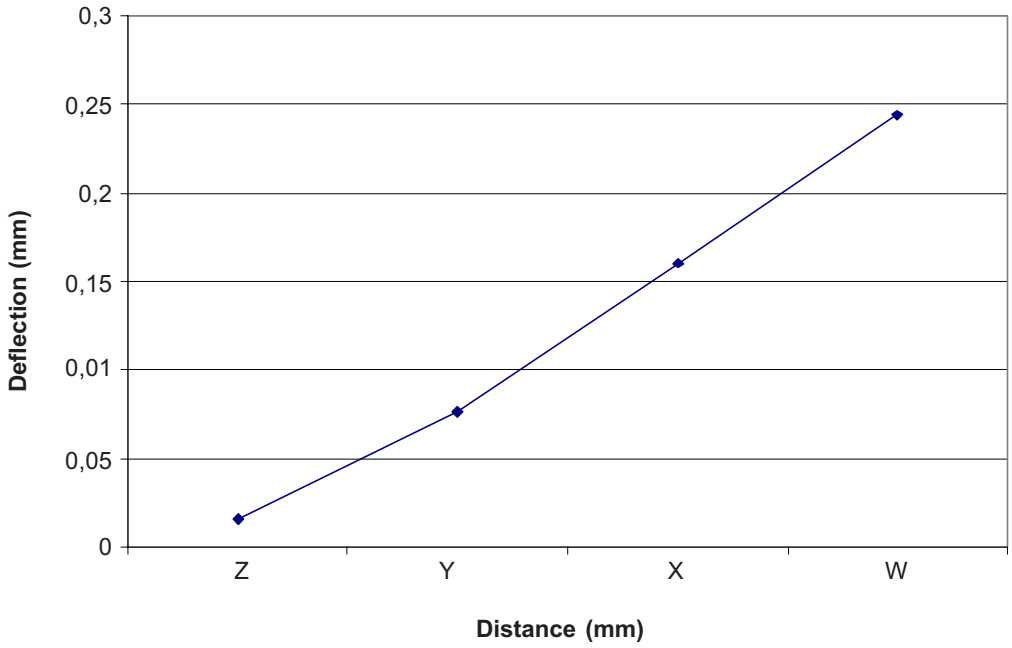

Figure 12 Deflection *vs.* Distance (AM1)

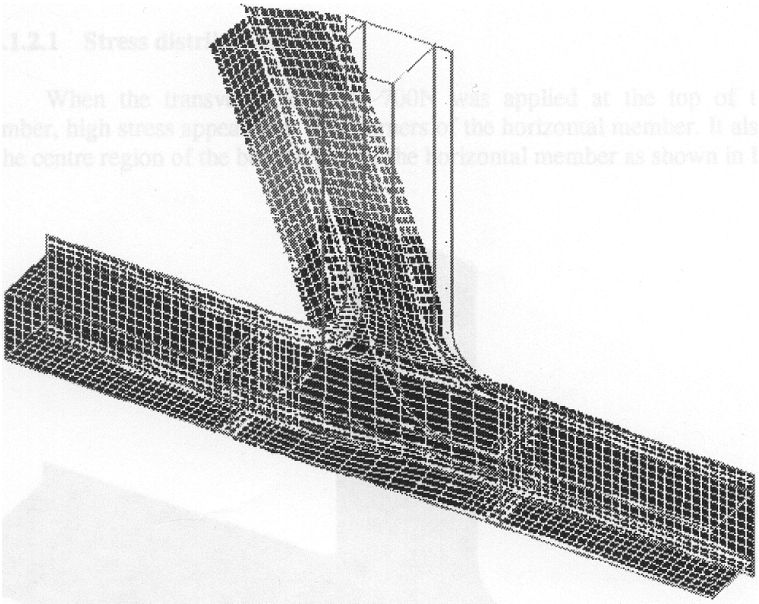

Figure 13 Deformed model for AM1

vertical member and the centre region of the horizontal member were largely deformed.

5.1.2 Model AM2

The stress distribution appeared in model AM2 is quite similar to AM1 when longitudinal of 900 N was applied at the top of the vertical member. The results as shown in Table 7 and Figure 14, the graph shows no negative displacement occurred and therefore no occurrence of local bending at the particular point of measurement. High stress appeared to be along the flanges at the corner radii region as shown in Figure 15.

Table 7 Results for model AM2

Location	W (456.6 mm)	X (358.9 mm)	Y(261.2 mm)	Z(143.6 mm)
Deflection	0.248	0.161	0.075	0.009

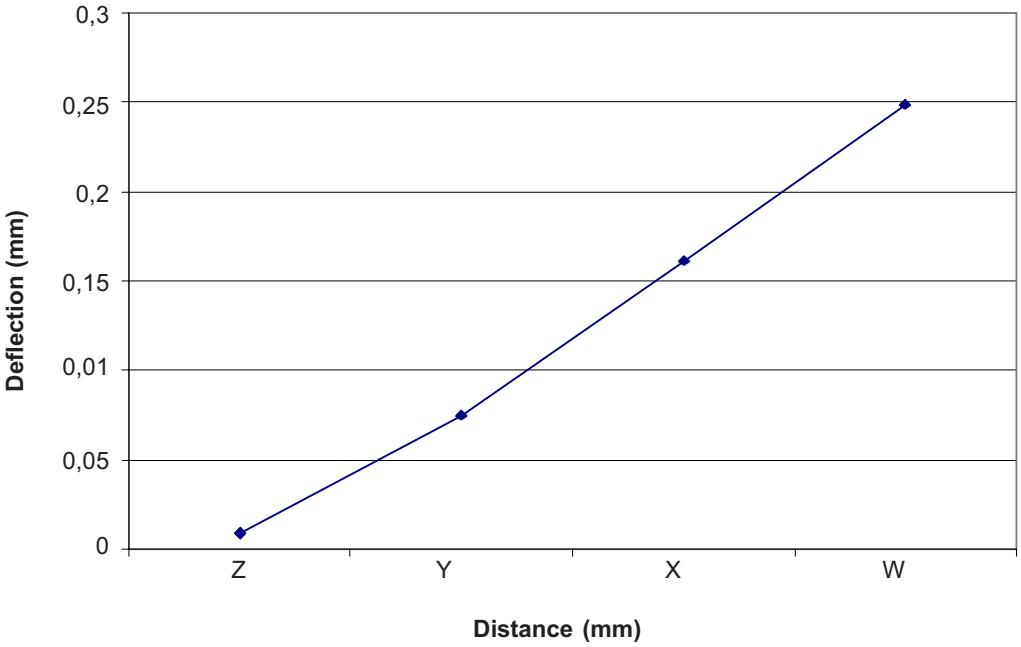

Figure 14 Deflection *vs.* Distance (AM2)

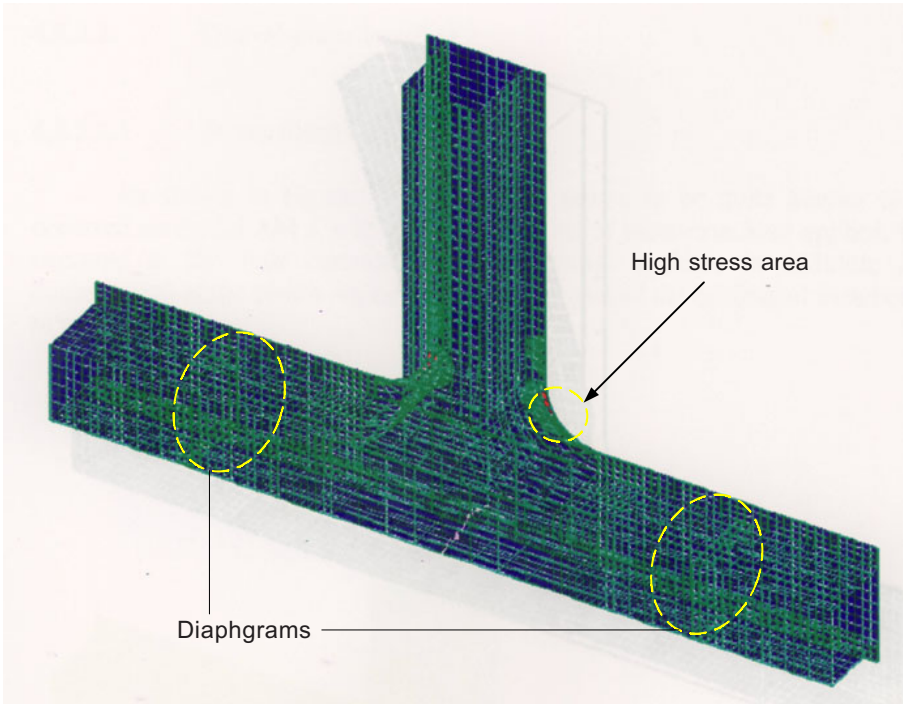

Figure 15 Stress distribution for model AM2

5.1.3 Model AM3

The results obtained from FE analysis for AM3 are shown in Table 8 and Figure 16. As refer to Figure 17, the stress for AM3 is concentrated along the flanges in the corner radii region. The model AM3 have inner diaphragms located in-line with the vertical line, therefore it prevents the model from being largely deformed at the centre region. However, it starts deformed immediately after the right inner diaphragms. Figure 17 shows deformed model for AM3.

Table 8 Results for model AM3

Location	W (456.6 mm)	X (358.9 mm)	Y(261.2 mm)	Z(143.6 mm)
Deflection	0.2503	0.1644	0.0807	0.0177

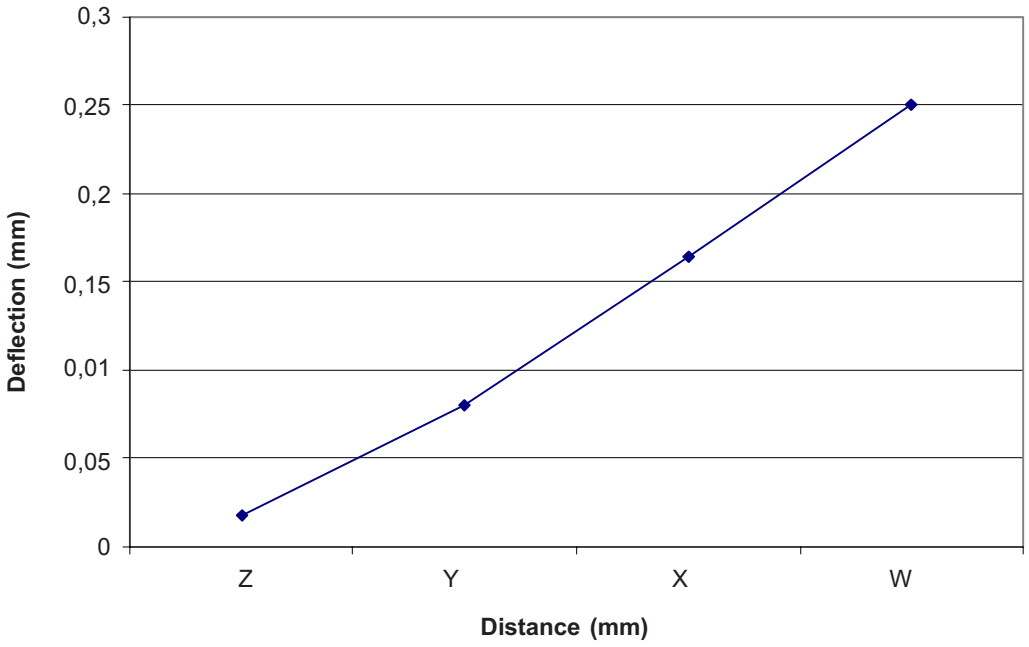

Figure 16 Deflection *vs.* Distance (AM3)

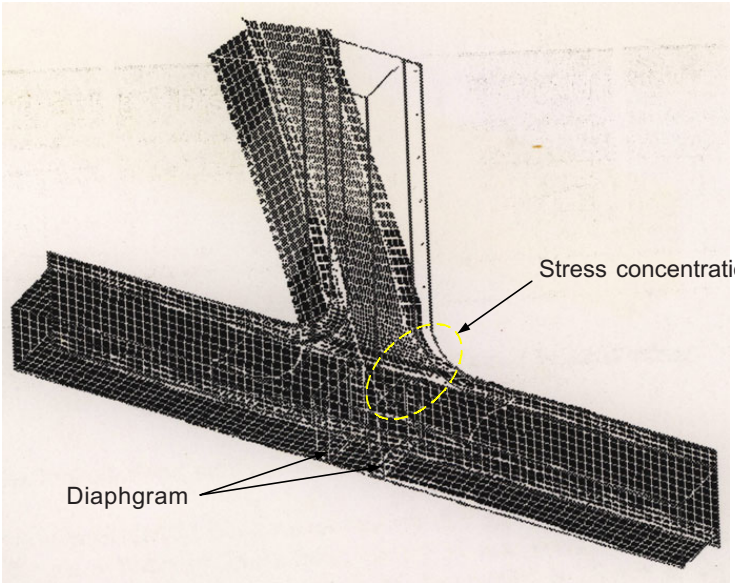

Figure 17 Deformed model and stress concentration area for AM3

5.2 Deflection of Vertical Member and Joint Region of Continuous Sill Member

The results obtained based on 900 N longitudinal load applied to T-flames structure in FE analysis have been tabulated in Table 9 and Figure 18.

Based on Table 9 and Figure 18, the following are the pre-conclusion that can be drawn.

(i) Model AM1 is stiffer than the other two models. However as the locations of measurement is nearer to the joint area, model AM2 shows that it is the stiffest among the models

(ii) No 'match box' effect occurred.

Table 9 Deflection of vertical member and joint region

Location	W (456.6 mm)	X (358.9 mm)	Y(261.2 mm)	Z(143.6 mm)
AM1	0.244	0.160	0.077	0.016
AM2	0.248	0.161	0.075	0.009
AM3	0.250	0.164	0.081	0.018

6.0 DISCUSSION

The results obtained from experimental analysis and finite element analysis has been tabulated in Table 10.

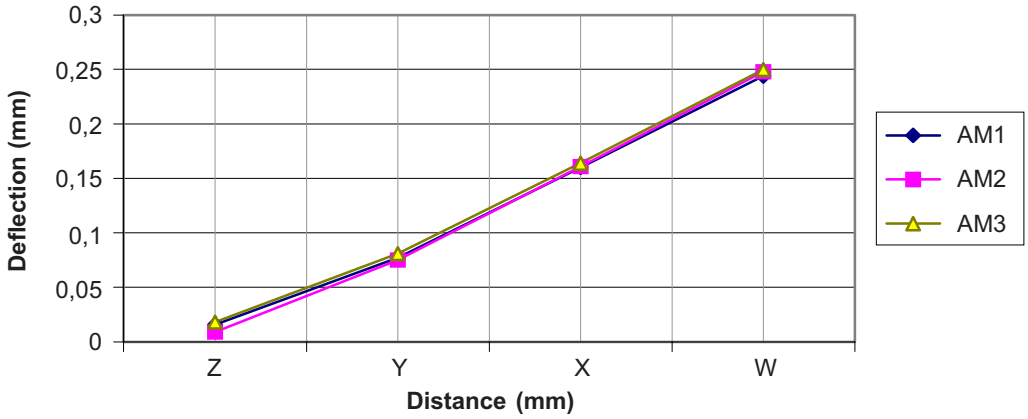

Figure 18 Deflection of vertical member and joint region of continuous sill member

From Table 10, it can be seen that the results obtained from FE analysis gave deflection within the range of 93% to 99% of the experimental test. There are differences of the results for both analyses especially at point Z. From FE analysis, there are no negative displacement occurred at point Z. These results seem to be contradicted with the results obtained from the experiment test but the reason can be found in the quality of the specimens. The result shows that specimen AM1 is stiffest model and AM2 is stiffer than AM3.

Table 10 Displacement of vertical member due to longitudinal load of 900 N

Location	Experimental Test			Finite Element Analysis		
	AM1	AM2	AM3	AM1	AM2	AM3
W	0.246	0.262	0.268	0.244 (99%)	0.248 (95%)	0.250 (93%)
X	0.162	0.174	0.189	0.160	0.161	0.164
Y	0.044	0.076	0.084	0.077	0.075	0.081
Z	–0.010	–0.008	–0.008	0.016	0.009	0.018

7.0 CONCLUSION

Based on the results obtained from the experimental work, location of diaphragms for the specimens do not gives any major influences for in-plane bending case due to the shape and direction baffles are not suitable. However, the specimen with diaphragms located at the weld line is stiffer than the other specimens.

Most side frames are constructed by a single outer pressing operation where the outer has section of the B-pillar and sill member are made in a single pressing. Therefore, the future experimental test should be considered on this type of frames. Although

there is no match box effect in the experimental and finite element testing, the further research can be made to improve the stiffness of the T-frame structure. The future work will be carrying out for out-of-plane bending as well as the non-continuous sill member.

REFERENCES

[1] McGregor, I. J., D. Nardini, Y. Gao, and D. J. Meadows. 1992. Development of A Joint Design Approach for Aluminium Automotive Structures. *SAE Technical Paper Series.* 922112: 1-13.

[2] Sunami, Y., T. Yugawa, and Y. Yoshida. 1998. Analysis of Joint Rigidity in Plane Bending of Plane-joint. *JSAE Review.* 9(2): 44-51.

[3] Sunami, Y., T. Yugawa, and Y. Yoshida. 1990. Analysis of Joint Rigidity of the Automotive Body Structure Out-of-plane Joint Structures. *JSAE Review.* 11(3): 59-66.

[4] Sharman, P. W. and A. Al-Hammoud. 1987. The Effect of Local Details on the Stiffness of Car Body Joints. *International Journal of Vehicle Design.* 8(4/5/6): 526-537.

[5] Niisawa, J., N. Tomioka, and W. Yi. 1984. Analytical Method of Rigidities of Thin-walled Beams with Spot Welding Joints and Its Application to Torsion Problems. *JSAE Review.* 11(3): 77-85.

[6] Vayas, I. and D. Briassoulis. 1993. Behavior of Thin-Walled Steel Frame Joints. *Journal of Constructional Steel Research.* 24(2): 105-119.

[7] El-sayed, M. E. M. 1989. Calculation of Joint Spring Rates Using Finite Element Formulation. *Computer and Structures.* 33(4): 977-981.

[8] Balch, C. D. and C. R. Steele. 1987. Asymptotic Solutions for Warping and Distortion of Thin-walled Box Beams. *ASME Journal of Applied Mechanics.* 54**:** 165-173.

[9] Altenbach, J. 1991. Finite Element Modelling and Analysis of Thin-walled Structures. *The Mathematics of Finite Elements and Applications VII London*, London: Academic Press.

[10] Altenbach, J., W. Kissing, and H. Altenbach. 1994. *Dunnwandige Stab-und Stabschalentragwerke Braunschweig*, Wiesbaden: Vieweg.

[11] Shakourzadeh, H., Y. O. Guo, and J. L. Batoz. 1999. Modeling of Connections in the Analyses of Thin-Walled Space Frames. *Computers and Structures.* 71(4): 423-433.

[12] Moon, Y. M., H. Lee, and Y. P. Park. 1999. Development of An Automotive Joint Model Using An Analytically Based Formulation. *Journal of Sound and Vibration.* 220(4): 625-640.

[13] Mirza, F. A., A. A. Shehata, and R. M. Korol. 1982. Modeling of Double Chord Rectangular Hollow Section T-joints by Finite Element Method. *Computers & Structures.* 15(2): 123-129.

[14] Cheng, W. and X. Deng. 2000. Performance of Shell Elements in Modelling Spot Joints. *Finite Elements in Analysis and Design.* 35: 41-57.